IBRACON Structures and Materials Journal
Revista IBRACON de Estruturas e Materiais
ISSN 1983-4195 ismj.org

ORIGINAL ARTICLE

Multi-objective optimization of outriggers in high-rise buildings subjected to wind loads

Otimização multiobjetivo de outriggers em edifícios altos submetidos a cargas de vento

Felipe Morrone Barbat Parfitt[a]
Inácio Benvegnu Morsch[a]
Herbert Martins Gomes[a,b]

[a]Universidade Federal do Rio Grande do Sul – UFRGS, Graduate Program in Civil Engineering, Porto Alegre, RS, Brasil
[b]Universidade Federal do Rio Grande do Sul – UFRGS, Graduate Program in Mechanical Engineering, Porto Alegre, RS, Brasil

Received 30 May 2022
Accepted 25 July 2022

Abstract: This paper aims to investigate a methodology for determining the optimum floor positioning of outriggers (ORs) and belt-trusses (BTs) over tall buildings height. The primary goal is to reduce the maximum lateral drift (MLD) and the core base moment (CBM), individually and concurrently. Furthermore, the influence of these elements on other criteria such as maximum acceleration and natural frequencies are analyzed. Throughout the work, the behavior of the structure is verified when the stiffness ratio of the main elements used in the bracing system (core, perimeter columns, OR, and BT) are varied. Therefore, a three-dimensional model of a tall building under lateral wind load is analyzed, using the finite element method with ANSYS software. The mono and multi-objective optimizations were solved, respectively, by the Nelder-Mead method with the author's modifications to deal with integer variables and by a utility function. Based on the results, it is concluded that by specifically adding ORs/ORs-BTs in tall buildings the influence on the reduction of the mentioned objectives is extremely relevant, reaching up to 68% for the CBM and 71% for the MLD, depending on the amounts employed.

Keywords: outrigger, tall buildings, structural optimization, integer programming, lateral load.

Resumo: Neste trabalho os autores têm por objetivo investigar uma metodologia para determinação dos pavimentos ótimos ao implementar outriggers (ORs) e belt-trusses (BTs) ao longo da altura de um edifício alto para reduzir tanto o máximo deslocamento lateral (MDL), quanto o momento na base do núcleo (MBN), de forma separada e concorrente. Além disso, analisa-se a influência destes elementos sobre outros critérios como a máxima aceleração e as frequências naturais. Ao longo do trabalho verifica-se o comportamento da estrutura quando a relação de rigidez dos principais elementos do sistema de contraventamento (núcleo, colunas perimetrais, OR e BT) são variados. Sendo assim, um modelo tridimensional de um edifício alto sob ação lateral de vento é analisado, empregando o método dos elementos finitos usando o software ANSYS. As otimizações mono e multiobjetivo foram resolvidas, respectivamente, pelo método Nelder-Mead modificado para variáveis inteiras pelos autores e pela função de utilidade. Diante dos resultados, conclui-se que ao introduzir de forma específica os ORs/ORs-BTs em edifícios altos a influência na redução dos objetivos mencionados é extremamente relevante, podendo chegar a 68% para o MBN e 71% para o MDL, dependendo de suas quantidades empregadas.

Palavras-chave: outrigger, edifícios altos, otimização estrutural, programação inteira, carga lateral.

How to cite: F. M. B. Parfitt, I. B. Morsch, and H. M. Gomes, "Multi-objective optimization of outriggers in high-rise buildings subjected to wind loads," *Rev. IBRACON Estrut. Mater.*, vol. 16, no. 2, e16203, 2023, https://doi.org/10.1590/S1983-41952023000200003

Corresponding author: Felipe Morrone Barbat Parfitt. E-mail: felipeparfitt@gmail.com
Financial support: The authors would like to acknowledge the financial support of CAPES and CNPq.
Conflict of interest: Nothing to declare.
Data Availability: The data that support the findings of this study are available from the corresponding author, Parfitt, F.M., upon reasonable request.

1 INTRODUCTION

Tall building constructions have been a global phenomenon in recent decades, as explained by their growing number, mainly, in the Asian continent [1]. Scarcity of land in large urban centers combined with the growing pace of urbanization in this period are factors that contributed to this fact. Hence, vertical solutions are considered the main and recognized options for accommodating the high population density, with a low impact on the environment [2].

However, skyscrapers are an engineering challenge, especially concerning structural design because they are highly sensitive to natural loads, such as lateral loads from wind and earthquakes. The intensity of these loads is directly proportional to the structure's height, i.e., as the buildings grow towards the sky, the control of structural behavior becomes more and more challenging. In this sense, the stability and stiffness criteria become more relevant than the strength criteria and thus control the design. Therefore, choosing the best structural system is a determining factor for reducing the amount of materials, as well as satisfying safety conditions related to normative criteria or even to fit architectural aesthetics [3].

Conventional structural systems - such as framed, composed of rigid cores, or a combination of both - are no longer an economical solution to mitigate lateral loads when the number of floors increases. Among the many possible solutions, the outrigger system is one of the most widely employed options in the last decades, due to its compatibility with contemporary high-rise buildings. The most important one is associated with the architectural issue due to the flexibility of the facades. Furthermore, for being employed on specific floors, they are already opportune to be combined with other projects (mechanical floors).

The outrigger system is composed of an internal system (rigid core) and an external system (perimeter columns), connected by a rigid element, known as outrigger (OR). Eventually, belts are added around the perimeter to provide connectivity between the external columns, known in the literature as belt-truss (BT). ORs and BTs, in principle, can be placed on any floor over the building's height. However, there are specific floors where their contribution is greater to ensure the control of certain objectives. The maximum lateral drift (MLD), as well as the core base moment (CBM), are both important objectives to be reduced to achieve an optimized design. Therefore, knowing their optimum floors is extremely relevant for designers.

This paper aims to investigate a methodology for determining the optimum floors when employing outriggers ORs/ORs-BTs over the tall building height to reduce both the maximum lateral drift and the core base moment, individually and concurrently. Furthermore, the influence of these elements on other criteria such as maximum acceleration and natural frequencies are analyzed.

1.1 Bibliographical review

Some of the ORs analysis and design literature includes an optimization task, in which objective functions are always linked to important design code criteria or economic aspects. Maximum lateral displacement, inter-story drift, core base bending moment, differential axial shortening between the core and the outer columns, and OR system volume are some of the factors that have been sought to be reduced, as shown in [4]–[8].

In a 400 m high reinforced concrete building, Park et al. [4] evaluated the optimal design of OR's structural system elements, namely the core, external columns, and the OR itself. They also included the best number of ORs and their placement. The solutions were found using a genetic algorithm, to minimize the volume of the structural system, which includes displacement constraints at the top of the building and bending stress at the core's base.

Moon [1] examined the OR system's structural performance in tall buildings with complex shapes, i.e., twisted, tilted, and tapered. For each shape, the impact of both the angle of variation of the façade and the total height of the structure was verified. The analysis was performed using commercial software (SAP 2000). They demonstrate that: lateral stiffness decreases with increasing torsion rate, and as height increases, the stiffness reduction is more pronounced; it is more appropriate to employ columns away from the perimeter, reducing the thickness of the building, rather than twisted columns; in the case where the shape of the structure is tilted, when the tilted angle increases in a range from 0 to 13°, lateral wind strength increases and, on the other hand, lateral displacements due to gravity loads are intensified; structures that shorten along the height are more efficient under wind loads when the shortening angle or height increases.

Chen and Zhang [5] investigated a multi-objective genetic algorithm for ORs based on a reduced mathematical formulation. For 1 to 10 ORs, Pareto optimum solutions were found, i.e., many optimal positions based on the number of ORs. The top displacement and core base bending moment were the analysis' objectives.

Kim et al. [6] conducted a study using three tall structures, each having 80 floors (280 m) and vertical elements of various shapes, to determine the ideal position of the truss OR over the height that minimizes the maximum lateral drift.

In the optimization process, the gradient-descent approach was used, along with linear and quadratic interpolations. In addition, they verified the impact of the wind loading shape and the ideal position of the OR on the minimal bending moment at the core's base.

Kim et al. [7], considering the same model as [6], carried out a multi-objective optimization study trying to simultaneously reduce the maximum lateral displacement and the differential axial shortening, where the floors were the design variables. In order to solve the single and multi-objective optimization problem, they used the steepest descent method and the weighted-sum method, respectively. For the tall building model where the vertical elements stiffness changes over the height, they obtained the following results: the best floor to position one OR to minimize the maximum lateral displacement is at 47th, and for two, 27th and 57th floors; to minimize the differential axial shortening the best floor ORs are for one, 60th and, for two, 47th and 68th floor.

Xing et al. [8] conducted a study based on a seismic spectral analysis of a simplified model using buckling restrained braces (BRBs) OR system which is considered a damped OR. The authors themselves proposed and validated the model using the ANSYS program. To reach their goal, i.e., to obtain the optimal position of the damped OR and the corresponding structure top displacement, several structural parameters were varied. In this way, they concluded that: by increasing the OR stiffness, both objectives gradually decrease; by increasing the stiffness of the core of the columns, the OR's optimal position rises and the displacement decreases; when increasing the distance between the core and the columns, the OR's optimal position increases, and the displacement, at first, decreases quickly and, then, increases slowly; when increasing the BRB's yielding force, both objectives initially decrease and, then, remain unchanged. When comparing the results with those of the conventional OR, under the same conditions, they obtained both optimal location and the top displacement smaller.

The papers [5] and [6] perform a similar study attempting to obtain the set of optimal floors to minimize the same objective function (maximum lateral displacement). For [5] when there is only one OR its position should be 0.45 of the total height of the building (H), while for [6] this position should be $0.59H$. When there are 2 ORs throughout the height [5] defines that their positions should be $0.31H$ and $0.68H$, while for [6] they should be $0.35H$ and $0.71H$. Although both studies use a high-rise building with almost the same height and apply a similar wind profile, other different aspects can justify the disagreement between the results. Such differences are the simplified model analysis and the stiffness of the OR system elements, which interfere with the OR optimum positioning.

2 THEORETICAL BASIS

2.1 Tall building model

The tall building model used in the analyses of this study is based on Kim et al. [6], which is illustrated in Figure 1. It has 80 floors with a distance between floors of 3.5 m, which results in a total height of 280 m. Its floor plan format is regular and contains dimensions of 43×43 m. The distribution of the elements of the building structure is a central core, columns distributed around the perimeter, and beams and slabs between the inner and outer portions.

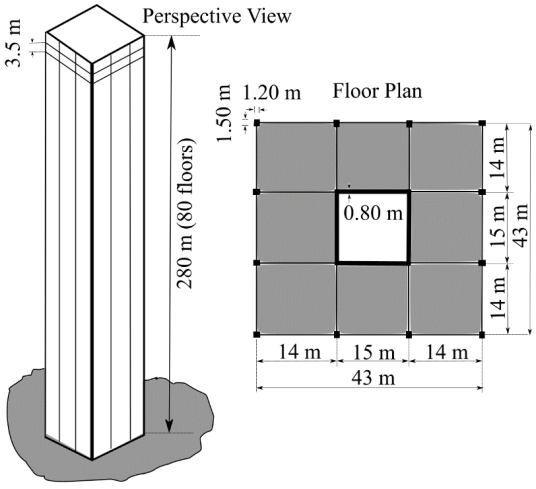

Figure 1. Tall building model

2.2 Dynamic effects of wind turbulence

The lateral wind loading was applied according to the methodology described in NBR 6123 [9]. For the development of the wind flow to excite a structure, the design speed $\overline{V}_P$, is calculated over a time period equal to 10 minutes, and it is given by

$$\overline{V}_P = 0.69 V_0 S_1 S_3, \tag{1}$$

where V_0 is the basic wind speed and the parameters S_1 and S_3 are the topographic and probabilistic factors, respectively. Since for each vibration mode j the total wind force at coordinate i can be calculated by the superposition of the mean force $\overline{X}_i$, and turbulence force $\hat{X}_i$, it results in

$$\tilde{X}_i = \overline{X}_i + \hat{X}_i. \tag{2}$$

The mean and turbulence forces are, respectively, given by

$$\overline{X}_i = \bar{q}_0 b^2 C_{ai} A_i \left(\frac{z_i}{z_r}\right)^{2p} \tag{3}$$

and

$$\hat{X}_i = F_H \Psi_i x_i \tag{4}$$

where $\bar{q}_0 = 0.613 \overline{V}_P^2$ is the reference height pressure, b and p are correction parameters according to the roughness category, z_r is the reference height (10 meters), F_H is the force referring to the turbulence plot -, C_{ai}, A_i, z_i, $\Psi_i = m_0/m_i$ and x_i are, respectively, the drag coefficient, wind force area, height, and ratio between the discrete mass (m_i) and the arbitrary reference mass (m_0), and the vibration mode - each one at the i coordinate.
The force referring to the turbulence component can be calculated according to

$$F_H = \bar{q}_0 b^2 A_0 \frac{\sum_{i=1}^{n} \hat{a}_i x_i}{\sum_{i=1}^{n} \Psi_i x_i^2} \hat{\imath} \tag{5}$$

where A_0 is the reference area, $\hat{\imath}$ is the dynamic amplification coefficient, n is the number of degrees of freedom considered in the discretization, and the parameter $\hat{a}_i$ is given by

$$\hat{a}_i = C_{ai} \frac{A_i}{A_0} \left(\frac{z_i}{z_r}\right)^p. \tag{6}$$

When more than one vibration mode is used in the solution, the result of the r modes can be combined by

$$\hat{Q} = \left[\sum_{j=1}^{r} \hat{Q}_j^2\right]^{1/2} \tag{7}$$

where $\hat{Q}_j$ can be any static or geometric variable (force, stress, strain).
The acceleration in mode j, induced by the turbulence forces, can be estimated by the following equation

$$a_j = 4\pi^2 f_j^2 \hat{u}_j \tag{8}$$

where f_j and $\hat{u}_j$ are, respectively, the frequency and the displacement due to the turbulence part at level z, both in mode j.

Since the tall building model is localized in the center of Porto Alegre (Category V), the basic speed is equal to $V_0 = 46\ m/s$. For being considered in a flat area and high occupancy factor, both correction factors, S_1 and S_3, were considered to be unitary. Considering that the model fits in category V, from Table 20 of NBR 6123 [9] the exponent $p = 0.31$ and the parameter $q = 0.5$ are assumed. From the model dimensions, the values $l_1/l_2 = 1$ and $H/l_1 = 6.5$ are obtained, which for a high turbulence wind provides a drag coefficient $Ca = 1.1$.

Taking into account that at each iteration of the optimization, the structure changes its configuration, the vibration mode x_i and the fundamental frequency f_j are constantly updated in APDL (Ansys Parametric Design Language) code. The vibration mode employed is calculated by the average of the displacements per floor, obtained through modal analysis. Furthermore, since the dynamic amplification coefficient ξ depends on the model's frequency, equations generated from Figure 18 of NBR 6123 [9] are generated by a degree-2 polynomial trend line when the damping ratio is equal to 2%.

2.3 Structural optimization

2.3.1 Problem formulation

The objective functions to be optimized in this work are: (a) the maximum lateral drift and (b) the core base bending moment. For such purposes, a set number of floors with ORs/ORs-BTs are introduced to each optimization, and then the result is obtained individually for each objective. The amount of design variables depends on the number of ORs that will be placed throughout the height of the tall building. The formulation of the first and second problems is given by:

Minimize:

$$f_1(\boldsymbol{x}) = \Delta_{top} \tag{9}$$

and

$$f_2(\boldsymbol{x}) = M_{core} \tag{10}$$

subject to

$$\boldsymbol{x} \in \mathbb{Z}^n,$$

$$x_{i,min} \leq x_i \leq x_{i,max}\ i = 1, \dots, n, \tag{11}$$

$$|x_i - x_{i+1}| \leq h_{or}\ i = 1, \dots, n-1;$$

where x are the design variables (floors with ORs/ORs-BTs), Δ_{top} is the normalized MLD, h_{or} is the OR height, $\mathbb{Z}^n$ is the set of integer variables, n is the number of design variables, $x_{i,min}$ and $x_{i,max}$ represent the lower and upper limits, respectively, and M_{core} is the normalized CBM, which is calculated by the resultant of the sum of bending moments around the axes forming the plane of the core's base.

The minimization of each of these problems is performed by using the Nelder-Mead algorithm modified in this paper for integer variables, which is presented in subsection 2.3.2. The constraints are handled through the penalty method. It is noteworthy that the bounds are defined according to the number of floors and also by the number of floors that a single OR/OR-BT comprises. In this case, as presented in Chapter 3, the lateral bounds are from the 4th to the 80th floor, and to avoid overlapping of ORs/ORs-BTs, the height difference between ORs/ORs-BTs must always be larger than 4 floors.

2.3.2 Nelder-Mead algorithm modified for integer design variables

Introduced by Nelder and Mead [10], Nelder-Mead is a numerical method that aims to minimize or maximize mathematical functions. According to Arora [11], it is a direct search method that does not use gradients in its solution procedure and can solve optimization problems with nonlinear functions. Its approach is based on the comparison of

the values of the objective function of $n+1$ vertices of a geometric configuration known as Simplex, where n is the number of design variables. In the case of a function with only two variables, the problem is considered two-dimensional, with the Simplex being a triangle formed by three vertices.

At each iteration of the Nelder-Mead algorithm, one seeks to improve the worst vertex of the Simplex through some operations - reflection, expansion, or contraction. The worst result function perturbation is always in the mean direction of the remaining points. If none of the operations results in an acceptable point, all vertices are approached in the direction of the best particle [12]. However, it was verified through benchmark functions that this procedure is very susceptible to being stuck in local minima and, therefore, the global minimum is not obtained. For this reason, algorithm modifications will be proposed here to avoid undesirable situations in the optimization process.

The modified Nelder-Mead algorithm shown below follows the same step-by-step as described by the original version, as referred at [12]. However, in this case, it will be introduced: (a) randomizations in each of the operations mentioned above; (b) a new operation when all particles are identical. Only particles with integer variables are aimed at dealing with integer programming problems. Always at the beginning of each iteration, all particles are arranged in ascending order so that

$$f(\boldsymbol{x_1}) \leq f(\boldsymbol{x_2}) \leq \cdots \leq f(\boldsymbol{x_{n+1}}) \tag{12}$$

and therefore, the centroid can be calculated according to:

$$\overline{\boldsymbol{x}} = \frac{1}{n}\sum_{i=1}^{n} x_i. \tag{13}$$

The first operation to be carried out is always the reflection and, depending on its result, other operations are performed. The mathematical expression that defines all operations mentioned is modified and takes the following form:

$$\boldsymbol{x} = round[\overline{\boldsymbol{x}}(1 + c_n \boldsymbol{R_{normal}}) + coef(\overline{\boldsymbol{x}} - \boldsymbol{x_{n+1}})], \tag{14}$$

where $round$ represents the rounding operation to the nearest integer number, $c_n = 0.1$ is the reducing coefficient, $\boldsymbol{R_{normal}}$ is a vector containing samples of a standard normal distribution (with mean 0 and standard deviation 1) and $coef$ varies according to the type of operation: in reflection $coef = 1$; in expansion $coef = 2$; in the external contraction $coef = 0.5$; in the internal contraction $coef = -0.5$.

If none of the operations improves the result of the objective function, retraction is applied, in which all particles approach the one with the best result. This can be calculated according to

$$\boldsymbol{x_i} = round\left[\boldsymbol{x_1} + \left(\frac{1}{2} + c_n \boldsymbol{R_{normal}}\right)(\boldsymbol{x_1} - \boldsymbol{x_i})\right] \ (i = 2, 3, \dots, n+1). \tag{15}$$

Furthermore, before applying the contraction, it is always checked if all vertices are identical, i.e.,$(\boldsymbol{x_1} = \boldsymbol{x_2} = \cdots = \boldsymbol{x_{n+1}})$. In case this condition is true, $\boldsymbol{x_1}$ is stored and then a random dilation is applied to $\boldsymbol{x_1}$, given by the expression:

$$\boldsymbol{x_i} = round(\boldsymbol{x_1} + c_d \boldsymbol{R_{normal}}) \ (i = 2, 3, \dots, n+1) \tag{16}$$

where $c_d = 0.5$ is the dilatation coefficient.

As previously stated, all the coefficients used in the operations are the same as those proposed by Nelder and Mead [10] in the original method. The ones included in the new programming, c_n and c_d, were chosen according to the best results obtained through tests on eight benchmark functions for integer variables.

Python programming language was used to connect the optimization code and the structural analysis performed by ANSYS APDL. Every time the objective function is evaluated, a computational cost of a few seconds is spent. Thus, to speed up this process, a database was created. This procedure allows that a value already in the database does not need to be evaluated twice in the optimization process, since the analysis for those design variables has already been performed previously. This was only possible due to the integer feature of the problem being optimized.

Finally, to validate the modified Nelder-Mead algorithm, the authors tested 8 benchmark functions for integer variables presented in [13]. In fact, the modifications developed in this paper were fundamental for the success of the algorithm, considering that seven out of the eight benchmark functions reached global minima in each campaign of independent runs, which would not have happened without those modifications. More details about the algorithm can be found in [14].

2.3.3 Utility function method

As previously defined, both objective functions, f_1 and f_2, participate in multi-objective optimization. The utility function method was chosen in this study because it allows the use of the previously designed mono-objective optimization algorithm for integer variables. This method assigns weights to each objective function, where the sum of the weights must be one. Therefore, it is possible to prioritize one of the objectives by increasing its weight in the optimization. Although according to Arora [11], this approach is the most common among the multi-objective optimization methods, as seen later, it converges to a defined number of optimum values as the weight step decreases.

So, the problem containing both objectives can be now defined as:

Minimize:

$$f_1(\boldsymbol{x}) = \omega f_1(x) + (1-\omega) f_2(x), \tag{17}$$

subject to

$$\boldsymbol{x} \in \mathbb{Z}^n,$$

$$x_{i,min} \leq x_i \leq x_{i,max}\ i = 1, \dots, n, \tag{18}$$
$$|x_i - x_{i+1}| \leq h_{or}\ i = 1, \dots, n-1;$$

where ω is the weight factor that ranges from 0 to 1.

According to Equation 17, it is possible to prove that by combining both objective functions, the problem becomes simpler and can be solved by a single-objective optimization algorithm. On the other hand, the convergence of this method depends on the weight discretization ($\Delta\omega$) assumed, which defines a distance between the set of weights in the search of several prioritizing assumptions for each objective. This will result in the so-called "Pareto Frontier", a set of all possible solutions, assuming diverse prioritizing weights. The number of weight factors employed in the equation can be calculated by $Np = 1/\Delta\,\omega + 1$, then the distribution will be $\Omega = \{0, \Delta\omega, 2\Delta\omega, \dots, 1\}$. It is worth noting at the moment when ω is equal to 0 or 1, it means that one of the objectives does not have any influence on the optimization. In this case, the problem behaves as a single-objective optimization, with its results being the extremes of the Pareto solutions. Since the frontier is made up of a fixed number, there will be a discretization limit for ω, which will imply not finding new solutions.

3 TALL BUILDING MODEL AND ANALYSIS

3.1 Tall building numerical model

The representation of a part of the numerical model in finite elements is shown in Figure 2. Note that to improve the visualization, the elements are represented with thickness, being: a concrete core with elasticity modulus $E = 3.96 \times 10^4\ MPa$, Poisson's ratio $\nu = 0.2$ and thickness of $t = 0.8\ m$; ORs and BTs of steel trusses with elasticity modulus $E = 210 \times 10^3\ MPa$, Poisson's ratio $\nu = 0.3$ and area ratio between the chord and web bars of $A_{web} = A_{chord}\sqrt{2}$, being their values defined later through a study; perimeter columns with elasticity modulus $E = 3.96 \times 10^4\ MPa$, Poisson's ratio $\nu = 0.2$ and cross section of $1.5 \times 1.2\ m$ (see Figure 2b for the spatial orientations); and steel beams with elasticity modulus $E = 210 \times 10^3\ MPa$, Poisson's ratio $\nu = 0.3$ and area of $A_v = 0.08\ m^2$. The total model mass is $7.71 \times 10^7\ kg$. An important aspect that can be observed from Figure 2a is that the OR and the BT cross 3 floors, and their positions correspond to the highest floor they are located on.

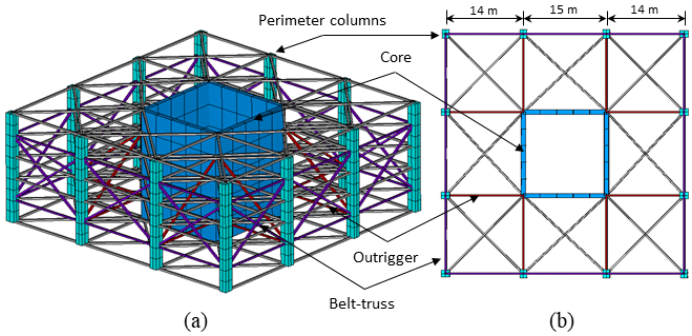

Figure 2. Numerical model in (a) perspective (b) plan.

The shell finite element (SHELL181) was used in the core, the truss element (LINK180) in the ORs, BTs, and floor beams, and the beam element (BEAM188) in the columns. According to a mesh study, the columns were discretized by two elements on each floor with a quadratic function and the core by twenty elements per floor. The building's base is fully fixed. It is worth noting that the truss elements placed on the floor simulate the rigid diaphragm promoted by the floor slabs, the same principle applied in other works, such as Lee and Tovar [15].

3.2 Tall building without outrigger/belt-truss analysis

3.2.1 Modal analysis

Modal analysis was used to determine the vibration modes and natural frequencies of the structure. Using the subspace iteration method, the first ten vibration modes or those that fit in a range of 0 to 2 Hz were extracted. Figure 3 illustrates the first six vibration modes of the structure.

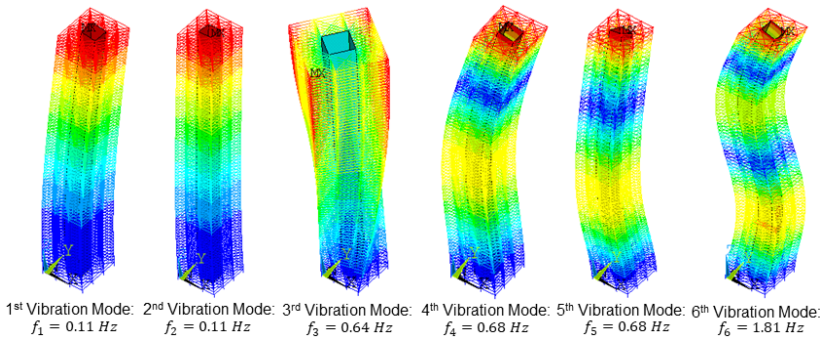

Figure 3. 1st to 6th tall building vibration mode without ORs-BTs.

As can be seen in Figure 3, for the first two modes, bending predominates, with the same frequency's values and perpendicular directions to each other, since the structure is symmetric. The 3rd mode is torsional, and the 4th presents bending characteristics with one node. Finally, the 5th mode is similar to the 4th, and the 6th mode, showing a bending mode with two nodes.

3.2.2 Static analysis

To obtain the maximum lateral drift and the core base bending moment of the structure when subjected to lateral wind loading applied according to section 2.2, a static analysis is performed. Additionally, maximum acceleration is determined.

3.2.2.1 Maximum lateral drift

The largest lateral drift is at the top and has a value of $0.7318\ m$. A result that compared to the overall building deflection limit of $H/500 = 0.56\ m$, is 30.7% higher and therefore must be controlled by a structural solution.

3.2.2.2 Core base bending moment

The core base bending moment, as already mentioned, is calculated by the resultant from the binaries and moments around the x and y axes, according to

$$M_{core} = \sqrt{\left(\sum M_x + \sum F_z d_y\right)^2 + \left(\sum M_y + \sum F_z d_x\right)^2} \tag{19}$$

where M_x and M_y are, respectively, the bending moments around x and y, d_x and d_y are, respectively, the variable distances in x and y from the point force F_z to its axis.

Based on the direction of all reactions at the core of the tall building model without ORs/BTs it is possible to calculate the resulting bending moment about the central point of the core, which is equal to $M_{core} = 2.3944 \times 10^3\ MN.m$, with more than 99% corresponding to the portion of the sum of $F_z dx$.

3.2.2.3 Maximum acceleration

The maximum acceleration, according to Equation 8, occurs on the floor with the largest lateral drift. Therefore, knowing that the maximum lateral drift for the first vibration mode due to the floating fraction is $0.2244\ m$, it follows that $a = 0.114\ m/s^2$. If compared to the human comfort criterion, such as the one for residential buildings of 1.5 to 2% of the gravity acceleration, which corresponds to $0.147\ m/s^2$, the acceleration obtained is lower and is also within this limit.

3.4 Tall building with outrigger/belt-truss analysis

In this section, the analyses of the numerical model using the outrigger system are presented. To evaluate the performance of the structure, the results of the objectives/criteria are verified as a couple of interest parameters are modified. In all cases, it is desired to minimize maximum lateral drift and the core base moment – and, concerning this criterion, to minimize maximum acceleration and maximize the natural frequencies.

3.4.1 Outrigger stiffness analysis

By increasing the OR stiffness, it is expected that the analyzed objectives follow an inversely proportional path, except in the case of the fundamental frequency, which must continue increasing. To verify the influence of the cross-sectional area of the OR in relation to the objectives, the horizontal member areas of the OR varied from 0 to $0.14\ m^2$. Figure 4 shows the best results found for each value of the adopted area, i.e., the OR is in the different optimum floors for each case of area.

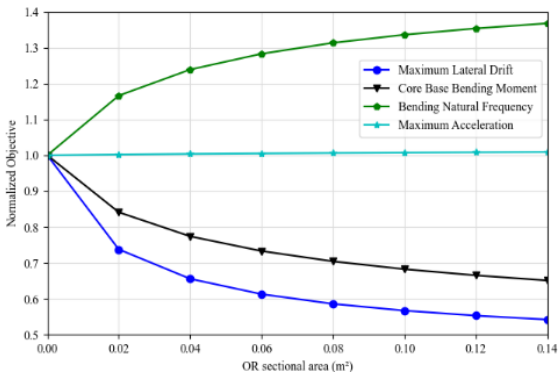

Figure 4. Influence of the OR area regarding the objectives/criteria analyzed.

Figure 4 shows that: (a) the influence of OR stiffness on the variation rate of the analyzed objectives, in absolute values, follows a decreasing trajectory; (b) there is a qualitatively constant relationship between the MLD and CBM; (c) after exceeding the OR cross-sectional area of $0.06\ m^2$ the objectives have a little change, with the largest variation of approximately 3%, which is possibly not justifiable in economic ways; and (d) the maximum acceleration shows an indifferent behavior with the OR area. Moreover, using an area of $0.06\ m^2$ for the horizontal bars of the OR, significant reductions of 39% for the MLD and 27% for the CBM are reached. For the bending natural frequency, there is an increase of 28%.

On the other hand, from Figure 5 it is worth emphasizing that the optimum OR positioning (given by the floor with the lowest value of the objective function) over the height of the model is variable according to the objective analyzed and also by the OR cross-section area. In general, the maximum lateral drift, the natural frequency, and the maximum acceleration have optimum floors close to each other, being located in the upper half of the building. Regarding the core base moment, the optimum floors are always located in the lower half. It is worth mentioning that by increasing the OR stiffness, the optimum floor decreases its location in all cases, i.e., it gets closer to the base. Another important point observed is the increasing OR capacity to redistribute the forces from the core to the perimeter columns as the OR stiffness increases, a fact verified by the CBM's curvature increment.

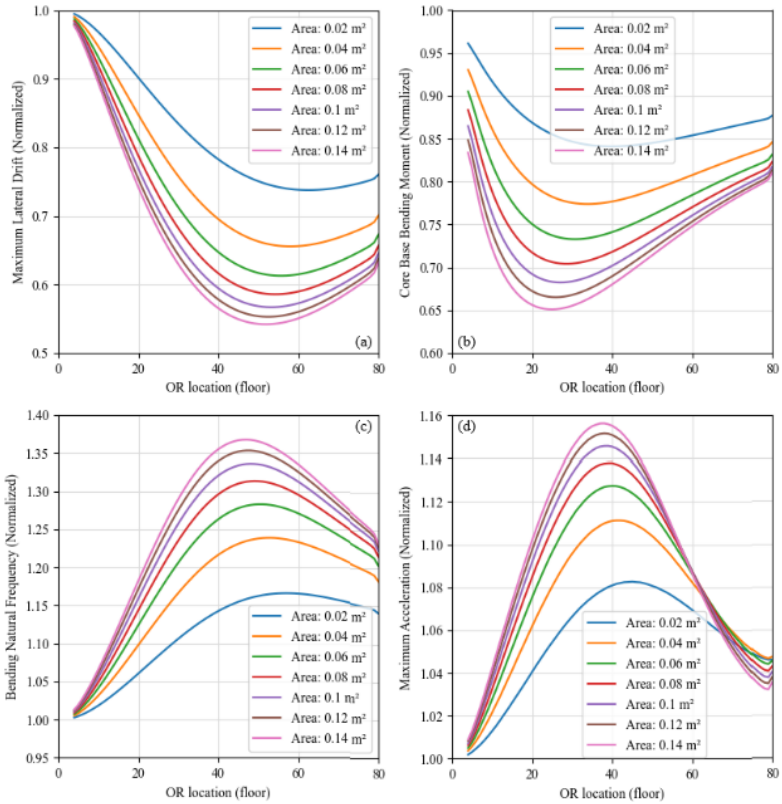

Figure 5. Influence of the OR area in relation to the optimum floor to (a) MLD (b) CBM (c) Bending nat. freq. (d) Max. accel.

3.4.2 Belt-truss stiffness analysis

An option to improve even more the tall building stiffness performance and also to take advantage of the available space of the mechanical floors is to implement a belt-truss around the perimeter of the floor where the OR is located. By joining the outer columns through the BT, not only those columns that are directly connected to the OR are going to support the intense lateral loads, but also all the others. Therefore, by adding this element to the lateral system, all the objectives analyzed should be modified, in order to improve the behavior of the building. The torsional stiffness of the building, which had not been checked in the previous analysis with ORs only, in principle, should also be benefited.

As in the case of subsection 3.4.1, at first the study is carried out by modifying the BT cross-section area from 0 to $0.14\ m^2$, to evaluate its influence on the structural behavior. The cross-section area ratio between the web and the chords is $\sqrt{2}$. Figure 6 shows the optimum results obtained for each value of BT area and analyzed objective function when there is only one OR.

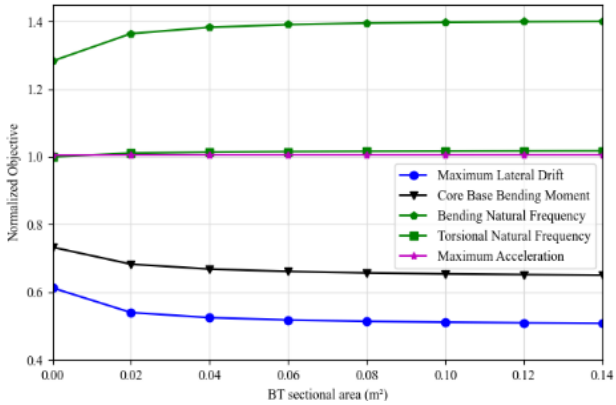

Figure 6. Influence of the BT area in relation to the objectives/criteria analyzed.

Figure 6 illustrates that by adding the BT together with OR, the analyzed objectives are smoothly improved, except for the torsional natural frequency and maximum acceleration, which remain almost constant. However, it is noticeable that the interference of the BT stiffness is almost imperceptible regarding any of the objectives. Another important point that should be highlighted is the null contribution of the BT on torsional stiffness, a parameter according to the studies that should be improved. Such a fact can be justified by the floor system used to simulate the rigid diaphragm of the slabs since the connection between the core and the outer columns through the truss elements does not allow the relative torsional strain between the outer and inner portions. Since the increase in the area of the BT does not reasonably affect the building's behavior, and for convenience, the same area ratio of the ORs is used, $A_{BT} = 0.06\ m^2$. Figure 7 illustrates for each objective the influence of the OR-BT concerning its location over height as well as the BT stiffness.

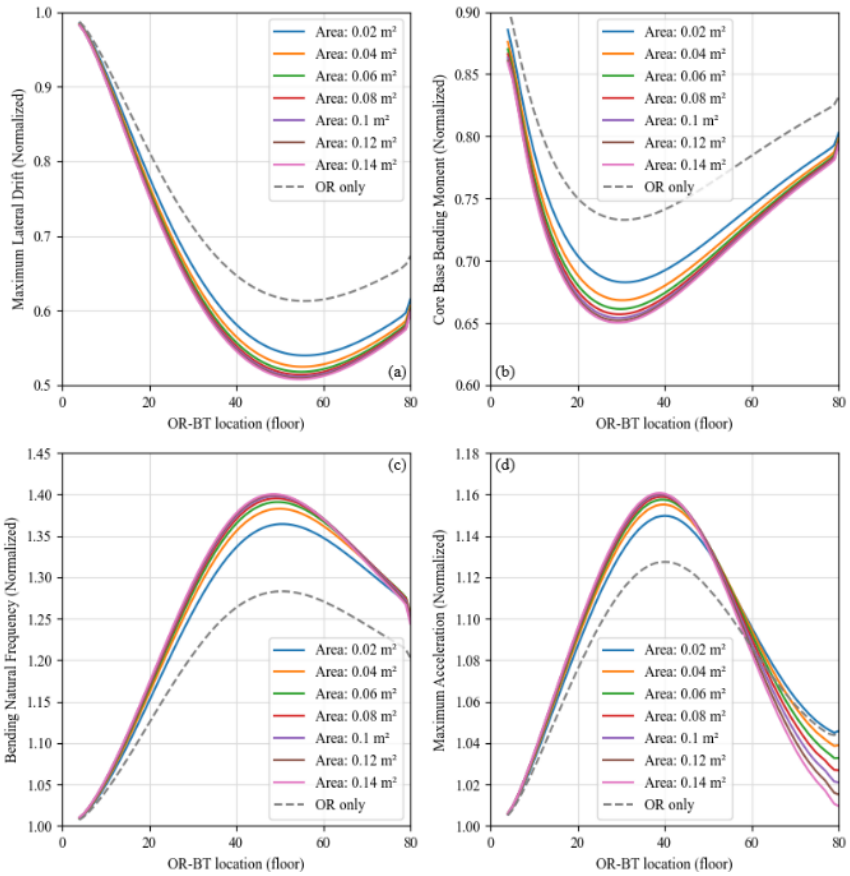

Figure 7. Influence of the BT area in relation to the optimum location to (a) MLD (b) CBM (c) Bending. natural freq. (d) Max. accel.

Observing Figure 7 it can be concluded that the BT area does not significantly affect the OR-BT optimum positioning. In fact, what happens is just a translation of the curve when there is only the OR.

3.4.3 Columns-core stiffness ratio analysis

Taking into consideration that the core and the outer columns are both components of the OR-BT lateral system and work together, possibly the stiffness ratio between these elements should affect the analyzed objectives. Thereby, to verify if this relationship is actually relevant to the study, the building response was calculated for several stiffness ratios (R_{rig}), whereas the equation for a single case is given by

$$R_{rig} = \frac{I_{cols}}{I_{core}} \tag{20}$$

where I_{core} and I_{cols} are, respectively, the area moment of inertia about the geometric center of the model for the core and the set of columns. Another important point is that in order to not prioritize any of the two elements, the standard model is used as a reference, i.e., the core or columns area value is modified in such a way that the sum of the areas remains always the same, regardless of the stiffness ratio. Additionally, to simplify the understanding, the stiffness ratio has been normalized from the standard model, which has $R_{rig} = 7.84$. Figure 8 shows the optimum results obtained for each stiffness ratio value and analyzed objective function when there is only one OR-BT.

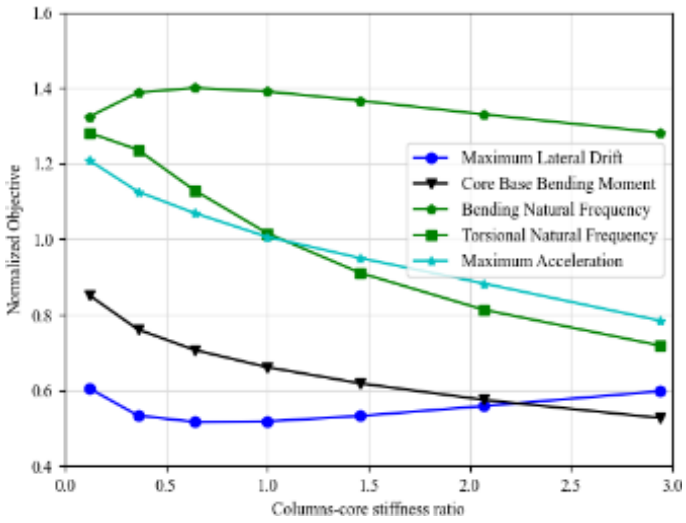

Figure 8. Influence of the column-core stiffness ratio on the objectives/criteria analyzed.

Based on Figure 8 it is proven that the stiffness ratio directly interferes with the model response. The maximum lateral drift and natural bending frequency curves show the existence of an optimum stiffness ratio ($0.36 < R_{rig} < 1$), which has a larger core area and, consequently, a smaller column area, when compared to the reference model. Regarding the core base moment, the lowest value is reached by increasing R_{rig}, so the outer columns are able to carry more axial load. The same behavior happens for the maximum acceleration. Meanwhile, for the torsional natural frequency the opposite happens, since the higher its value, the better the building response will be.

Figure 9 illustrates for each objective the influence of the OR-BT positioning as well as the stiffness ratio between the columns and the core.

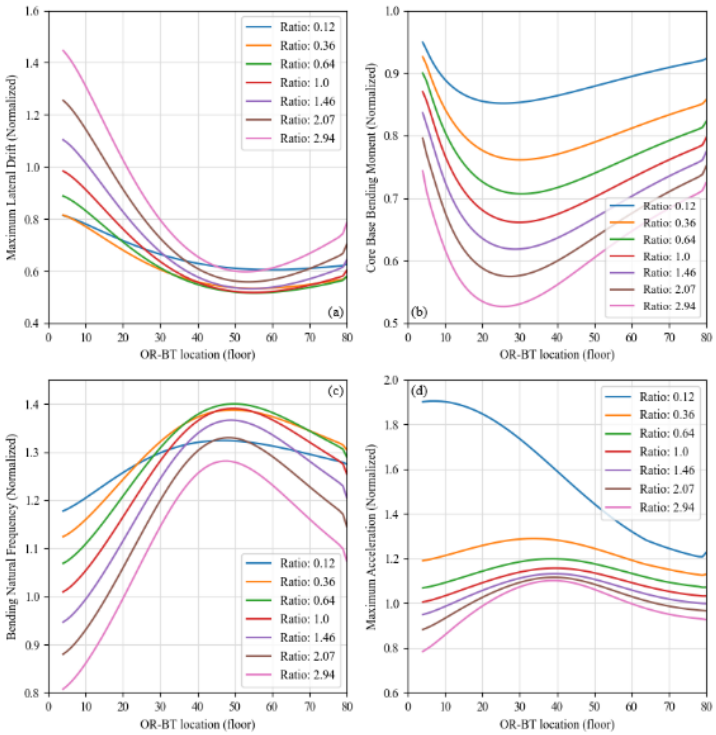

Figure 9. Influence of the column-core stiffness ratio on the optimum location to (a) MLD (b) CBM (c) Bending nat. freq. (d) Max. accel.

Analyzing Figure 9, at first, it is visible that when the stiffness ratio is low, the OR-BT becomes less effective, due to the small variation of the objectives by changing the position of the OR-BT. A different behavior occurs for the maximum acceleration when $R_{rig} = 0.12$, that from the 4th to 80th floors its value always decreases. As already highlighted for the MLD and natural bending frequency there is an optimum ratio that, for the cases studied, is $R_{rig} = 0.64$. Regarding the optimum floors, it should be noted the different stiffness ratio does not significantly change them, except for the CBM case.

4 STRUCTURAL OPTIMIZATION

4.1 Code validation

To prove that the modified Nelder-Mead algorithm is actually obtaining a global minimum, exhaustive searches were performed for three different cases: (i) a single-objective optimization considering 2 ORs being the objective of the CDM, as shown in Figure 10; (ii) a multi-objective optimization considering 2 ORs, as shown in Figure 11 (a); and (iii) a multi-objective optimization considering 2 ORs-BTs, as shown in Figure 11 (b). It is noteworthy that the graph in Figure 10 is symmetrical because there is no difference in the value of the objective function when the OR positioning is changed within the design variable. The presence of a continuous diagonal is merely illustrative, as both ORs cannot be present in the same position.

In the first exhaustive search illustrated in Figure 10, it is observed that the ideal floors to position the ORs are the 39th and 62nd. with a normalized result of 0.515, i.e., exactly the same values observed in the single-objective optimization. To obtain the optimal value when there are two ORs, regardless of the objective, using the modified Nelder-Mead it takes, on average, 30 iterations, against 2701 calls to the ANSYS program from the exhaustive search. This demonstrates, once again, the efficiency of the algorithm. Concerning the other two exhaustive searches carried out, it is concluded that both Pareto frontiers obtained through multi-objective optimization are correctly positioned, having, therefore, only non-dominated Pareto points to the others.

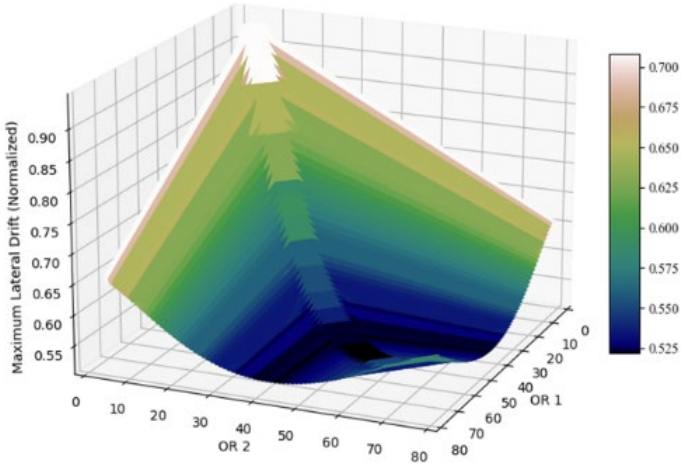

Figure 10. Exhaustive search with 2 ORs (Objective: MLD)

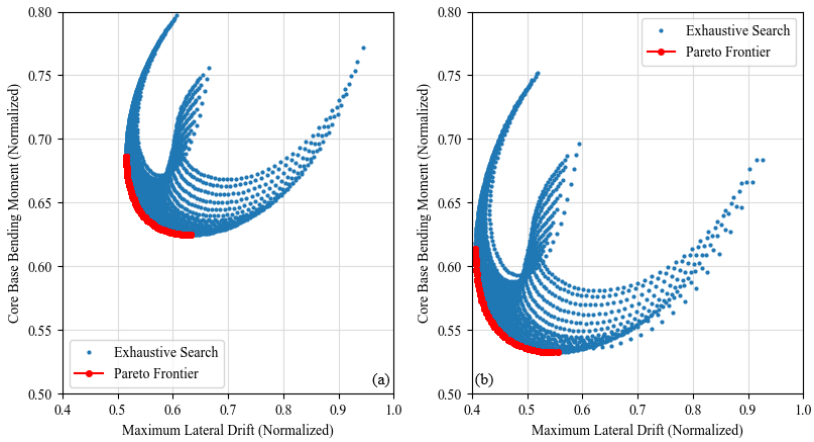

Figure 11. Exhaustive search with (a) 2 ORs (b) 2 ORs-BTs (compared to Pareto frontier obtained in this paper)

4.2 Single-objective optimization

The result of the single-objective optimization is obtained using the modified Nelder-Mead algorithm, adopting the same parameters as in subsection 2.3.2.

4.2.1 Maximum lateral drift

Table 1 and Table 2 show the optimum positions obtained to minimize the maximum lateral drift of the model presented in Chapter 3, with their respective results normalized by the values without ORs-BTs, which are: MLD of $0.732\,m$, CBM of $2.3944 \times 10^3\,MN.m$, fundamental frequency of $0.11\,Hz$, and maximum acceleration of $0.114\,m/s^2$. Table 1 presents the results of the optimizations with ORs only, and Table 2 with ORs and BTs.

Table 1. Results of single-objective optimizations for MLD (OR)

Number of ORs	Optimum floor	MLD	CBM	Fundamental freq.	Max. accel.
		norm.	norm.	norm.	norm.
1	56	0.613	0.775	1.279	1.098
2	39, 62	0.515	0.686	1.398	1.13
3	32, 47, 66	0.469	0.637	1.468	1.144
4	27, 39, 52, 68	0.442	0.601	1.515	1.155
5	24, 34, 44, 56, 70	0.423	0.576	1.549	1.161
6	21, 29, 38, 47, 58, 71	0.41	0.551	1.576	1.168

Table 2. Results of single-objective optimizations for MLD (OR-BT)

Number of ORs-BTs	Optimum floor	MLD	CBM	Fundamental freq.	Max. accel.
		norm.	norm.	norm.	norm.
1	55	0.518	0.717	1.384	1.115
2	39, 62	0.406	0.614	1.562	1.157
3	31, 47, 66	0.355	0.553	1.672	1.185
4	30, 34, 51, 68	0.325	0.512	1.754	1.213
5	26, 30, 47, 51, 69	0.304	0.481	1.815	1.234
6	23, 27, 40, 44, 57, 70	0.289	0.454	1.862	1.249

It can be noted that by introducing at least one OR, the reduction of lateral displacement is already extremely relevant, with approximately a 39% reduction. As the amount of ORs increases, the displacement reduction also continues to increase, but at a lower rate. When there are six ORs, the reduction percentage reaches 59%. By adding the BT to the model, the reduction in MLD is even greater, from 48% for one OR-BT and 71% for six OR-BT. For the two models analyzed, with OR and OR-BT, both the CBM and the bending natural frequency improve with the addition of new ORs/ORs-BT and, on the other hand, the maximum acceleration worsens. It is also noteworthy that the optimum floors for both cases are very similar.

4.2.2 Core base bending moment

Table 3 and Table 4 show the optimum positions obtained to minimize the core base moment in the tall building model, with their respective results normalized by the values without ORs-BTs. Like the MLD, the CBM follows the same pattern, always improving the objectives by increasing the amount of ORs or ORs-BTs, except in the case of maximum acceleration. In the first case, with ORs only, by introducing one OR in the model, a 27% reduction in CBM is achieved, and when there are six ORs, 55%. In the second case, with ORs and BTs, with one OR-BT the reduction is 34% and with six ORs-BTs, 68%.

Table 3. Results of single-objective optimizations for CBM (OR)

Number of ORs	Optimum floor	CBM	MLD	Fundamental freq.	Max. accel.
		norm.	norm.	norm.	norm.
1	31	0.733	0.704	1.214	1.116
2	17, 34	0.625	0.632	1.287	1.143
3	11, 19, 35	0.56	0.603	1.32	1.154
4	8, 12, 20, 36	0.514	0.585	1.341	1.161
5	4, 9, 13, 21, 36	0.476	0.577	1.352	1.164
6	4, 8, 12, 26, 23, 37	0.446	0.554	1.382	1.174

Table 4. Results of single-objective optimizations for CBM (OR-BT)

Number of ORs-BTs	Optimum floor	CBM	MLD	Fundamental freq.	Max. accel.
		norm.	norm.	norm.	norm.
1	30	0.661	0.637	1.281	1.139
2	16, 33	0.534	0.555	1.379	1.172
3	12, 16, 34	0.452	0.524	1.422	1.184
4	4, 8, 18, 34	0.404	0.523	1.424	1.184
5	4, 8, 12, 16, 35	0.348	0.504	1.451	1.191
6	4, 8, 12, 16, 20, 36	0.316	0.465	1.515	1.212

Initially, the reduction in the MLD objective is more pronounced than the CBM. However, as the number of ORs increases, a smoothing happens in both curves, which converges to close results, as can be seen in Figure 12. Between the two objectives, the MLD has a greater reduction, with a tendency that if more than six ORs are used, the CBM will be lower. Comparing the optimum positions for both objectives, it can be said that the CBM always results in positions at floor levels below, regardless of the number of ORs.

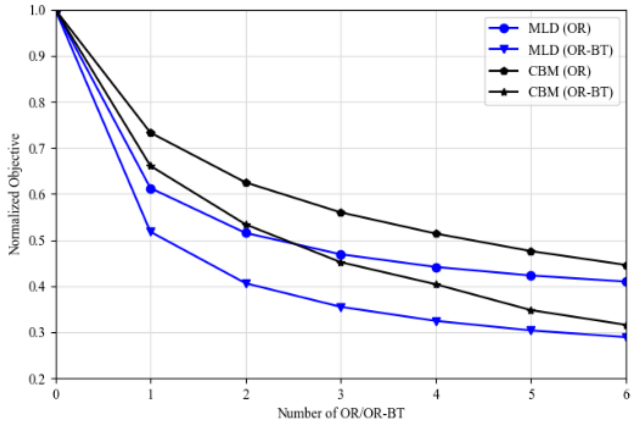

Figure 12. Result of each objective according to the number of OR/OR-BT

As already mentioned, adding the BT to the model helps to improve even more the main objectives. In this sense, it should be noted that it is possible to add fewer ORs over the building's height if there is a BT in the solution, as can be seen in the two cases presented in Figure 12. Given the MLD curves, it is possible to state that the solution with one OR-BT is equivalent to two ORs and the solution with two ORs-BTs is equivalent to six ORs. A similar situation happens with the CBM where, for example, three ORs-BTs are equivalent to six ORs. Moreover, adding ORs/ORs-BTs to the design of high-rise buildings implies an increase in execution time as well as in the project's final cost. Although such elements can be combined with mechanical floors, it must be carefully evaluated if this solution allows constructive and economical viability.

4.3 Multi-objective optimization

Each weight applied in Equation 17 provides only one optimum point on the Pareto frontier. Thus, it is necessary to discretize the weight in a small enough interval to obtain convergence in the results, that is, all Pareto solutions. Table 5 and Table 6 show the number of optimum positions according to the weight discretization ($\Delta\omega$) when the model has ORs and ORs-BTs, respectively. When the algorithm obtains the same number of solutions on the Pareto frontier in two consecutives $\Delta\omega$, the stopping criterion is reached.

Table 5. Number of optimal positions according to the weight discretization (ORs)

Number of ORs	$\Delta\omega$						
	0.1	**0.05**	**0.025**	**0.0125**	**0.00625**	**0.004**	**0.002**
1	11	19	26	26	-	-	-
2	11	21	32	39	41	42	42

Table 6. Number of optimal positions according to the weight discretization (ORs-BTs)

Number of ORs-BTs	$\Delta\omega$							
	0.1	**0.05**	**0.025**	**0.0125**	**0.00625**	**0.004**	**0.002**	**0.001**
1	11	19	26	26	-	-	-	-
2	11	21	32	37	39	41	42	42

As can be seen in Table 5, the minimum weight discretization, $\Delta\omega$, to reach all points of the frontier for one and two ORs are, respectively, 0.025 and 0.004. When the BT is added to the model, according to Table 6, the discretization for one OR-BT remains the same, and when there are two OR-BTs, $\Delta\omega$ decreases to 0.002. The extreme points of the Pareto frontier are the results of single-objective optimization. In the case of the optimization with one OR, the extreme positions are floors 31 and 56, resulting in exactly 26 points found. Therefore, even if $\Delta\omega$ was decreased, the number of positions would be the same. A similar behavior happens in the other cases.

Figure 13 illustrates all Pareto frontier points for both one and two ORs, as well as one and two ORs-BTs. It can be seen that the range of results for the MLD is more noticeable than for the CBM. In other words, CBM has a smaller variance compared to CBM. As already shown, the introduction of the BT causes an even greater reduction in the objectives. Another important point observed is the proximity of the frontier of two ORs and one OR-BT, which proves the efficiency of the BT and possibly exposes a feasible solution.

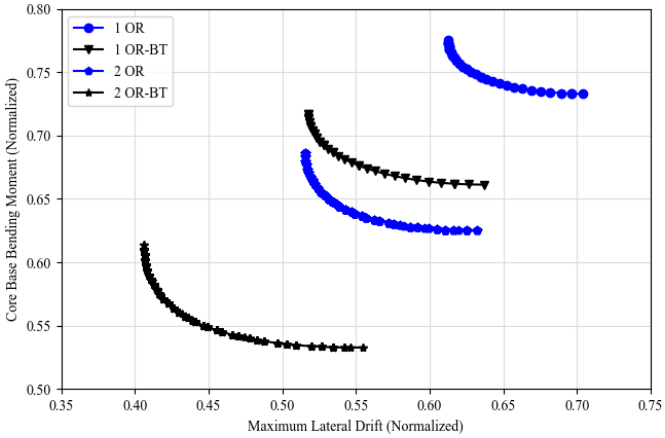

Figure 13. Pareto frontier for 1 and 2 ORs/ORs-BTs

All the optimum positions obtained through the optimizations can be seen in Table 7.

Table 7. Optimum positions resulting from multi-objective optimization

Number of ORs-BTs	Optimum positions
1 OR	all floors from the 31st to the 56th;
2 ORs	(17, 34); (17, 35); (17, 36); (18, 36); (18, 37); (18, 38); (18, 39); (19, 39); (19, 40); (19, 41); (19, 42); (20, 42); (20, 43); (20, 44); (21, 45); (21, 46); (22, 47); (22, 48); (23, 49); (23, 50); (24, 51); (25, 52); (25, 53); (26, 53); (26, 54); (27, 54); (27, 55); (28, 55); (28, 56); (29, 56); (29, 57); (30, 57); (31, 58); (32, 58); (32, 59); (33, 59); (34, 60); (35, 60); (36, 61); (37, 61); (38, 62); (39, 62);
1 OR-BT	all floors from the 30th to the 55th;
2 ORs-BTs	(16, 33); (16, 34); (17, 34); (17, 35); (17, 36); (17, 37); (18, 38); (18, 39); (18, 40); (19, 41); (19, 42); (19, 43); (20, 43); (20, 44); (20, 45); (21, 46); (21, 47); (22, 48); (22, 49); (23, 50); (23, 51); (24, 51); (24, 52); (25, 52); (25, 53); (26, 54); (27, 55); (28, 56); (29, 56); (29, 57); (30, 57); (30, 58); (31, 58); (32, 58); (32, 59); (33, 59); (34, 60); (35, 60); (36, 61); (37, 61); (38, 62); (39, 62);

All of the optimum floors presented above can be chosen to reduce the MLD and the CBM. However, if the designer wants to minimize one of the objectives more than the other, the choice must be made by observing the positions of the ORs/ORs-BTs along the height of the building. When the objective to be prioritized is the MLD, among all the options the best combination is the one with the floors positioned close to the top and, when it is the CBM, at the bottom. For example, for a tall building with two ORs-BTs and the priority is to reduce the CBM, the ORs positions should be as close as possible to the 16th and 33rd floors.

5 CONCLUSIONS

In view of the results and optimizations performed, this work proposed an algorithm and methodology to indicate the outriggers (ORs) or outriggers-belt-trusses (ORs-BTs) optimum positioning to minimize the maximum lateral drift (MLD) and the core base bending moment (CBM) in tall buildings under the action of lateral wind loads, as well as the influence of the implementation of these elements on maximum acceleration and natural frequencies. To this end, a tall building was modeled using the finite element method by the ANSYS program, and, using the Nelder-Mead algorithm, modified by the authors, the optimum positions were determined.

The comparison between the analysis results for the building with and without ORs/ORs-BTs proves that this bracing system is very efficient, considering the design criteria reductions. It is noticed that the optimal floors are different for each objective. In the MLD case, these floors are located more at the top. When there is only one OR/OR-BT, it is close to $0.7H$ and, when new elements are added, they are distributed along the height. In the CBM case, the floors are located at the bottom, regardless of the number of ORs/ORs-BTs. When there is one OR/OR-BT, it is at $0.37H$, and when new elements are added, they are distributed along the bottom in a range of $0.05 - 0.46H$. Kim et al. [6], considering a similar simplified model and adopting the building top drift as the objective function, obtain the optimal floor for one OR of $0.59H$. Difference of 16% in relation to that obtained in the present study, which can be justified by the presence of different stiffness in the elements of the OR system and wind loading profile.

It is noteworthy that for the tall building model used in the analyses, the solution with one OR would already be sufficient to be within the overall building deflection criterion since the element allows a reduction of about 39%. If necessary, it would be possible to reduce up to 60% of the lateral drift if six ORs were added in their optimal positions. On the other hand, if CBM were more important, introducing one OR could reduce it by 27%, or 55% with six ORs.

The advantage of including BT into the system is to reduce even more both main objectives by using fewer floors along the height. This solution allows the MLD to be reduced by 48% with one OR-BT, the same value obtained with two ORs. If two ORs-BTs were added the reduction would be 60%, which is equivalent to six ORs. A similar situation occurs with CBM, where three ORs-BTs are equivalent to six ORs.

The study carried out by varying the stiffness ratio between the external columns and the rigid core proves that there is a certain optimal ratio depending on the objective of interest. To obtain an optimal arrangement concerning the MLD, and based on the tall building model, it would be necessary to increase the core stiffness and decrease the stiffness of the column. The opposite is valid when the objective is the CBM. In this second case, in fact, it would be necessary to implement a constraint, because by increasing the ratio, the objective always continues to decrease.

The multi-objective optimization result provides engineers with several options to position ORs/ORs-BTs according to their interests. Such that choosing the best floor combination, fitting certain design considerations and specific objectives, is not conditioned to the extremes of the Pareto frontier (result considering only one objective), but close to it, with little interference in its optimal value.

ACKNOWLEDGEMENTS

The authors thank CNPq (National Council for Scientific and Technological Development) and CAPES (Coordination for the Improvement of Higher Education Personnel) for their support to this research.

REFERENCES

[1] K. S. Moon, "Outrigger systems for structural design of complex-shaped tall buildings," *Int. J. High-Rise Buildings*, vol. 5, no. 1, pp. 13–20, Mar 2016, http://dx.doi.org/10.21022/IJHRB.2016.5.1.13.

[2] K. S. Moon, "Why tall buildings? The potential of sustainable technologies in tall buildings," *Int. J. High-Rise Buildings*, vol. 1, no. 2, pp. 117–123, Jun 2012, http://dx.doi.org/10.21022/IJHRB.2012.1.2.117.

[3] M. H. Gunel and H. E. Ilgin, "A proposal for the classification of structural systems of tall buildings," *Build. Environ.*, vol. 42, no. 7, pp. 2667–2675, Jul 2007, http://dx.doi.org/10.1016/j.buildenv.2006.07.007.

[4] H. S. Park, E. Lee, S. W. Choi, B. K. Oh, T. Cho, and Y. Kim, "Genetic-algorithm-based minimum weight design of an outrigger system for high-rise buildings," *Eng. Struct.*, vol. 117, pp. 496–505, Jun 2016, http://dx.doi.org/10.1016/j.engstruct.2016.02.027.

[5] Y. Chen and Z. Zhang, "Analysis of outrigger numbers and locations in outrigger braced structures using a multiobjective genetic algorithm," *Struct. Des. Tall Spec. Build.*, vol. 27, no. 1, e1408, Aug 2018, http://dx.doi.org/10.1002/tal.1408.

[6] H.-S. Kim, Y.-J. Lim, and H.-L. Lee, "Optimum location of outrigger in tall buildings using finite element analysis and gradient-based optimization method," *J. Build. Eng.*, vol. 31, pp. 101379, Sep 2020, http://dx.doi.org/10.1016/j.jobe.2020.101379.

[7] H. S. Kim, H. L. Lee, and Y. J. Lim, "Multi-objective optimization of dual-purpose outriggers in tall buildings to reduce lateral displacement and differential axial shortening," *Eng. Struct.*, vol. 189, pp. 296–308, Jun 2019, http://dx.doi.org/10.1016/j.engstruct.2019.03.098.

[8] L. Xing, Y. Zhou, and W. Huang, "Seismic optimization analysis of high-rise buildings with a buckling-restrained brace outrigger system," *Eng. Struct.*, vol. 220, pp. 110959, Oct 2020, http://dx.doi.org/10.1016/j.engstruct.2020.110959.

[9] Associação Brasileira de Normas Técnicas, *Wind Loads on Buildings*, ABNT NBR 6123, 1988. (in Portuguese).

[10] J. A. Nelder and R. Mead, "A Simplex method for function minimization," *Comput. J.*, vol. 7, no. 4, pp. 308–313, Jan 1965., http://dx.doi.org/10.1093/comjnl/7.4.308.

[11] J. S. Arora, *Introduction to Optimum Design*, 4th ed. London, UK: Elsevier, 2017.

[12] J. Nocedal and S. Wright, *Numerical Optimization*, 2nd ed. New York, NY, USA: Springer Sci. Bus Media, 2006.

[13] F. Luchi and R. A. Krohling, "Differential evolution and nelder-mead for constrained non-linear integer optimization problems," *Procedia Comput. Sci.*, vol. 55, pp. 668–677, Jul 2015, http://dx.doi.org/10.1016/j.procs.2015.07.071.

[14] F. M. B. Parfitt, “Otimização multiobjetivo de outriggers em edifícios altos submetidos a cargas de vento,” M.S. thesis, Dept. Civ. Eng., Univ. Fed. Rio Grande do Sul, Porto Alegre, 2022.

[15] S. Lee and A. Tovar, "Outrigger placement in tall buildings using topology optimization," *Eng. Struct.*, vol. 74, pp. 122–129, Jun 2014, http://dx.doi.org/10.1016/j.engstruct.2014.05.019.

Author contributions: FMP: conceptualization, writing, data curation; HMG: data curation, conceptualization, supervision, revision; IBM: supervision, methodology, conceptualization, formal analysis, revision.

Editors: Bernardo Horowitz, Guilherme Aris Parsekian.